Protein specific N-glycosylation of tyrosinase and tyrosinase-related protein-1 in B16 mouse melanoma cells

Gabriela NEGROIU*, Norica BRANZA-NICHITA*, Andrei J. PETRESCU*, Raymond A. DWEK† and Stefana M. PETRESCU*[1]

*Institute of Biochemistry, Romanian Academy, Splaiul Independentei 296, 77700 Bucharest 17, Romania, and †Oxford Glycobiology Institute, Department of Biochemistry, University of Oxford, South Parks Road, Oxford OX1 3QU, U.K.

Tyrosinase and tyrosinase-related protein-1 (TRP-1) are two melanogenic enzymes that regulate melanin biosynthesis. Both are glycoproteins and belong to the *TRP-1* gene family. They share a significant level of sequence similarity in several regions, including the catalytic domain and the potential N-glycosylation sites. We have recently shown that inhibition of the early steps of N-glycan processing in B16F1 cells dramatically affects tyrosinase activity and melanin synthesis. We present here results on N-glycan processing of TRP-1 and tyrosinase and compare the maturation process and activity of both glycoproteins in the presence of inhibitors of the endoplasmic reticulum stages of N-glycosylation.

N-glycan analysis reveals that each of these two glycoproteins contains a mixture of high-mannose and sialylated complex N-glycans. However, in contrast to TRP-1, tyrosinase presents a homogeneous high-mannose glycoform, also.

In the presence of α-glucosidases inhibitors, the maturation of tyrosinase N-glycans is completely inhibited, whereas TRP-1 is still able to acquire some complex glycans, indicating that endomannosidase acts preferentially on the later glycoprotein. In addition, the dopa-oxidase activity of tyrosinase is totally abolished, whereas for TRP-1 it is only partially affected. The results suggest that despite their structural similarity, tyrosinase is more sensitive than TRP-1 to perturbations of early N-glycan processing, in terms of maturation and catalytical activity.

Key words: dopa-oxidase activity, endomannosidase, protein folding, melanogenesis, *N*-butyldeoxynojirimicin, TRP-1.

INTRODUCTION

Melanogenesis is a complex metabolic pathway controlled by a family of enzymes known as tyrosinase-related proteins (TRPs), which are localized in the melanosomal membrane [1]. The TRPs share several structural properties, including a cytoplasmic and a transmembrane domain, a glycosylated lumenal domain including the cysteine-rich epidermal growth factor ('EGF') motif and two metal-binding regions involved in the structure of the catalytic site [2]. Tyrosinase (monophenol, L-dopa : oxygen oxidoreductase, EC 1.14.18.1) and TRP-1 are two members of this family. Whereas tyrosinase is the key enzyme of melanogenesis, TRP-1 is the most abundant glycoprotein expressed in melanocytes.

Tyrosinase catalyses the rate-limiting step in melanin synthesis, the hydroxylation of tyrosine to dopa. It also catalyses the second step, dopa oxidation to dopa-quinone [3]. The function of TRP-1 is not yet very well understood. It has been suggested that TRP-1 may be involved in the regulation of the distal reactions of melanogenesis, which control the quality of melanin polymer [4].

The main activity of TRP-1 in murine melanocytes is the oxidation of a major intermediate in melanogenesis, namely 5,6-dihydroyindole-2-carboxylic acid to indole-5,6-quinone-carboxylic acid [5]. However, this oxidase activity has not been confirmed for the human TRP-1, despite its 98 % homology with mouse TRP-1 [6]. It has been reported that the protein from murine melanoma cells also has a low dopa-oxidase activity [7], and that the two bands with dopa-oxidase activity separated by non-reducing SDS/PAGE actually correspond to TRP-1 and tyrosinase [8].

Both enzymes are glycoproteins, and six of their potential N-glycosylation sites are highly conserved among TRPs [9]. N-glycosylation sites are occupied co-translationally in the endoplasmic reticulum (ER) by $Glc_3Man_9GlcNAc_2$ (G3M9) [10]. The first two steps of N-glycan processing consist in the trimming of G3M9 to G1M9 by α-glucosidases I and II, in ER [11]. G1M9 glycans attached to the glycoprotein chain are recognized by calnexin, a lectin involved in glycoprotein folding [12]. In the presence of α-glucosidase I inhibitors, the trimming of the first glucose is abolished [13]. Thus the glucosylated glycans cannot be further processed and glycoprotein folding cannot be controlled by the calnexin cycle. However, in many cell lines this glucosidase blockade is overcome by a Golgi endomannosidase which trims the glucosylated glycoprotein to the $Man_8GlcNAc_2$ glycoform, allowing further processing to hybrid and a complex glycan structures, as would normally happen without the blockade [14].

We have recently shown that inhibition of α-glucosidase I by *N*-butyldeoxynojirimicin (NB-DNJ) in B16 melanoma cells results in the inactivation of tyrosinase and a dramatic loss of cell pigmentation [15]. Despite being functionally inactive, tyrosinase is surprisingly still targeted to the melanosomes, but it fails to initiate melanin biosynthesis. Experimentally, it has been shown

Abbreviations used: TRP, tyrosinase-related protein; NB-DNJ, *N*-butyldeoxynojirimicin; EndoH, endoglycosidase H; PNGaseF, peptide: N-glycosidase F; ER, endoplasmic reticulum; αPep7, rabbit anti-tyrosinase antibody; αPep1, rabbit anti-TRP-1 antibody; g.u., glucose units; LEMT, lower electrophoretically migrating tyrosinase; HEMT, higher electrophoretically migrating tyrosinase; M_x, an oligomannosidic structure with *x* mannoses; A(1–4), the number of antennae linked to the trimannosyl core; G(0–4), the number of terminal galactose residues in the structure; B, bisecting GlcNAc; S, sialic acid; GxMy, $Glc_xMan_yGlcNAc_2$.

[1] To whom correspondence should be addressed (e-mail stefana.petrescu@biochim.ro).

that a small dopa-oxidase activity of approx. 5% still persists in the treated cells [15]. One possibility is that TRP-1 rather than tyrosinase may be responsible for the remaining dopa-oxidase activity in NB-DNJ-treated cells.

In the present report we compare the N-glycan processing of tyrosinase and TRP-1 in B16 mouse melanoma cells and the relationships between maturation and activity in these two glycoproteins. We show that, as a result of the inhibition of early steps of N-glycosylation, tyrosinase is synthesized in an inactive form while the dopa-oxidase activity of TRP-1 is only slightly reduced. Moreover, whereas tyrosinase glycans remain unprocessed in NB-DNJ-treated cells, in the case of TRP-1 the glucosidase blockade is bypassed and the protein is able to acquire some complex N-glycans.

EXPERIMENTAL

Reagents, antibodies and enzymes

Aristar grade ammonia solution and formic acid were purchased from BDH–Merck (Poole, Dorset, U.K.). HPLC grade acetonitrile was purchased from Romil (Cambridge, U.K.). The NB-DNJ was from Searle–Monsanto (St. Louis, MO, U.S.A.) and the protease inhibitor cocktail containing leupeptin, aprotinin, sodium EDTA, bestatin, 4-(2-aminoethyl)benzenesulphonyl fluoride ('AEBSF') and E-64 was from Sigma. All other reagents were of the highest purity commercially available. The rabbit anti-tyrosinase (αPep7) and anti-TRP-1 (αPep1) antisera [7,16] were a generous gift from Dr. V. J. Hearing (National Institutes of Health, Bethesda, MD, U.S.A.) Peroxidase-labelled goat anti-(rabbit IgG) was from Sigma. *Arthrobacter urefaciens* sialidase (EC 3.2.1.18, acylneuraminyl hydrolase), bovine testis β-galactosidase (EC 3.2.1.23, β-D-galactoside galactohydrolase), jack-bean β-*N*-acetylhexosaminidase (EC 3.2.1.52, β-*N*-acetyl-D-hexosaminide *N*-acetylhexosaminohydrolase) and jack-bean α-mannosidase (EC 3.2.1.24, α-D-mannoside mannohydrolase) were obtained from Oxford GlycoSciences (Abingdon, Oxon., U.K.). Endoglycosidase H (EndoH) [EC 3.2.1.96, glycopeptide-D-mannosyl-N^4-(*N*-acetyl-D-glucosaminyl)$_2$-asparagine 1,4-*N*-acetyl-β-glusaminohydrolase] and peptide: N-glycosidase F (PNGase) [EC 3.5.15.2, N-linked-glycopeptide-(*N*-acetyl-β-D-glucosaminyl)-L-asparagine amidohydrolase] were from New England Biolabs (Beverly, MA, U.S.A.).

Cell culture

B16 F1 mouse melanoma cells and Chinese Hamster Ovarian (CHO) cells (European Collection of Animal Cell Cultures, Porton Down, U.K.) were cultured in RPMI 1640 medium (Life Technologies, Paisley, Scotland, U. K.) containing 10% (v/v) foetal calf serum (Sigma), 50 units/ml penicillin and 50 mg/ml streptomycin (Life Technologies). The cells were maintained at 37 °C in an atmosphere of air/CO_2 (19:1).

Expression of tyrosinase in CHO cells

The tyrosinase expression vector was a kind gift from Dr. Gunter Muller (German Cancer Research Center, Heidelberg, Germany). The plasmid pHDmcTyr1 was transfected into CHO cells using All Trans IT™ (Pan Vera, Madison, WI, U.S.A.) as transfection reagent. Cells were lysed in 10 mM phosphate buffer, pH 6.8, containing 1% Nonidet P40 and proteinase inhibitors, and the supernatant was obtained by centrifugation at 11000 ***g*** for 30 min.

Dopa-oxidase assay

The dopa-oxidase assay measures the conversion of dopa into dopachrome via dopaquinone [3]. This reaction is followed spectrophotometrically at 475 nm by the chromogenic appearance of dopachrome from 1 mM dopa. The assay was performed in 0.1 M phosphate buffer, pH 6.8. Detection of dopa-oxidase activity in gels was performed using dopa as a substrate [17].

Pulse–chase experiments

B16 mouse melanoma cells were harvested with EDTA, washed three times with 0.1M PBS, pH 7.2, and resuspended in methionine- and cysteine-free RPMI 1640 medium (Life Technologies), supplemented with 1% dialysed foetal calf serum. Cells (10^7 cells/ml) were preincubated in the presence or absence of 1mM NB-DNJ for 2 h before the addition of [^{35}S]methionine/[^{35}S]cysteine (Tran^{35}S-label, specific radioactivity 1100 Ci/mmol, from ICN Flow, Thame, Oxfordshire, U.K.) at 200 μCi/ml for the indicated pulse time. Following the labelling period, isotope-supplemented medium was removed, and cells were washed in RPMI medium containing unlabelled 5 mM methionine. At the indicated times, the chase media was removed and the cells were harvested by scraping into ice-cold PBS. After harvesting and washing with PBS, cells were lysed in 0.5 ml lysis buffer [50 mM Hepes, pH 7.5, containing 2% (w/v) CHAPS, 200 mM NaCl and proteinase inhibitors].

Immunoprecipitations

^{35}S-labelled cell lysates were precleared with 20 μl Protein A–Sepharose (Pharmacia Biotech) for 1 h at 4 °C and incubated with αPep7 or αPep1 antisera for 1 h at 4 °C. The immune complexes were separated by incubation with 20 μl Protein A–Sepharose for 1 h at 4 °C. The slurry was washed once in 50 mM Hepes, pH 7.5, containing 0.5% CHAPS and 200 mM NaCl, and once in water. Tyrosinase and TRP-1 were further digested with EndoH.

In depletion experiments melanosomal lysates obtained as described [15] were depleted of tyrosinase by immunoprecipitation as follows. αPep7 antiserum was incubated with the melanosomal lysate for 1 h at 4 °C and with Protein A–Sepharose for a further 1 h at 4 °C. The resultant supernatant was reincubated with a fresh pool of αPep7 antiserum and Protein A–Sepharose. The procedure was repeated until no tyrosinase was detected in the supernatant by Western blotting with αPep7 antiserum.

EndoH and PNGaseF digestions

^{35}S-labelled samples were digested with EndoH as follows. Tyrosinase or TRP-1 was eluted from the Protein A–Sepharose slurry in EndoH-denaturing buffer (0.5% SDS, 1% 2-mercaptoethanol) by incubation for 5 min at 100 °C. Samples were cooled and mixed with 1/10 concentrated EndoH reaction buffer (0.5 M sodium citrate, pH 5.5). To one half of the amount of each sample 500 units EndoH (1 μl) was added, and the other half of each sample (non-digested controls) contained EndoH buffer alone. Digested samples together with non-digested controls were incubated for 18 h at 37 °C.

In Western-blotting experiments cell lysates containing 20 μg protein were denatured in the EndoH- or PNGaseF-denaturing buffer for 5 min at 100 °C, cooled and mixed with 1/10 concentrated EndoH (0.5 M sodium citrate, pH 5.5) or PNGaseF

[0.5 M sodium phosphate, pH 7.5, containing 10 % (v/v) Nonidet P40] reaction buffers. Samples were digested with 500 units EndoH or 500 units PNGase for 18 h at 37 °C.

Electrophoresis and Western blotting

SDS/PAGE was performed in 7.5 % or 10 % (w/v) acrylamide gels under reducing or non-denaturing conditions. In reducing conditions samples were incubated for 5 min at 100 °C with SDS/PAGE sample buffer containing 2-mercaptoethanol. In non-denaturing conditions samples were mixed just before running with SDS/PAGE sample buffer without 2-mercaptoethanol.

For Western blotting, lysates were separated by electrophoresis under reducing conditions, transferred to Immobilon membranes (Millipore) and reacted with αPep7 or αPep1 antibodies. Visualization of antibodies was performed using the ECL® system (Amersham, Arlington Heights, IL, U.S.A.).

Glycan analysis

Tyrosinase and TRP-1 were separated by SDS/PAGE (7.5 %, w/v, acrylamide) in non-denaturing conditions and the bands with dopa-oxidase activity were excised from gel and further purified by affinity chromatography using nitrocellulose-immobilized antibodies as previously described [18]. Glycans released by hydrazinolysis were labelled at their reducing ends with the fluorescent dye 2-aminobenzamide from the Signal TM Labelling Kit (Oxford GlycoSystems) according to the manufacturer's instructions. Fluorescently labelled glycans (1–10 pmoles) were incubated with various exoglycosidases in the appropriate buffer in a final volume of 30 μl for 1–24 h at 37 °C. The solution was then heated for 5 min at 95 °C, spotted on to a nitrocellulose filter (Ultrafree NC, Millipore, Watford, U.K.) filtered by centrifugation and the filter washed twice with 15 μl 5 % (v/v) acetonitrile. The digested glycans were further analysed by HPLC. Normal-phase HPLC was carried out using a GlycoSep-N column (4.6 mm × 250 mm, Oxford GlycoSystems). Oligosaccharide separation was achieved by using a five-segment gradient as reported [19].

RESULTS

Analysis of tyrosinase and TRP-1 N-glycans

Tyrosinase and TRP-1 from B16 melanoma cells have been purified as described above. The N-glycans were released by hydrazinolysis, fluorescently labelled, then analysed by normal-phase HPLC directly or after digestion with mixtures of exoglycosidases [19]. The columns were calibrated for glucose units (g.u.) elution positions using a mixture of glucose oligomers in a standard dextran hydrolysate.

As shown in Figure 1(A), more than 12 major peaks were resolved in the sample containing tyrosinase N-glycans. The elution positions of the peaks are consistent with the following structures: A3G3S (9.0 g.u.), A3G3S2 (9.7 g.u.), A3G3S3 (10.2 g.u.), A3G3S4 (10.5 g.u.), A4G4S3 (10.6 g.u.), M9 (9.6 g.u.), M8 (8.9 g.u.), M7 (7.9 g.u.), A2G2S (7.6 g.u.), A2G2B (7.3 g.u.), M6 (7.1 g.u.), A2G2 (7.15 g.u.), M5 (6.2 g.u.). These assignments were confirmed in experiments using digestion with arrays of exoglycosidases (Figures 1B and 1C). Digestion with sialidase results in the peaks between 9.8–10.5 g.u. subsequently running at 9.7 g.u. (A4G4) and 8.3 g.u (A3G3), and the 7.6–7.7 g.u. peak (A2G2S + A2G2BS) subsequently running at 7.15 g.u (A2G2) and 7.3 g.u. (A2G2B) (Figure 1B). Digestion with a mixture of sialidase and β-galactosidase resolves three new peaks, at 5.5, 5.9 and 6.6 g.u.. These correspond to A2G0, A3G0 and A4G0 structures, respectively (Figure 1C). Digestion with sialidase + β-galactosidase + *N*-acetylhexosaminidase confirmed the polylactosamine structures. Finally, digestion with the mixture, sialidase + β-galactosidase + *N*-acetylhexosaminidase + mannosidase, showed that peaks at 6.3, 7.1, 7.9, 8.9 and 9.6 g.u in Figure 1(A) correspond to the high-mannose series M5, M6, M7, M8 and M9. The compositions of tyrosinase N-glycans are summarized in Table 1.

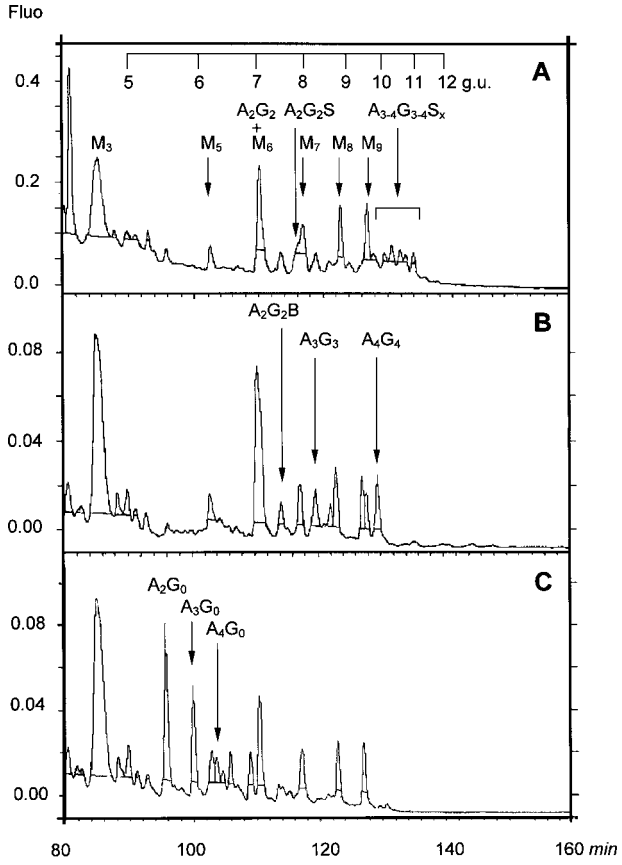

Figure 1 HPLC analysis of N-linked tyrosinase oligosaccharides digested with glycosidic enzyme arrays

N-linked tyrosinase glycans (**A**) were digested with sialidase (**B**) and sialidase + β-galactosidase (**C**). Oligosaccharides were digested for 3 h at 37 °C and analysed by normal-phase HPLC as described in the Experimental section. The *y* axis represents the fluorescence (Fluo) of the labelled glycans (excitation at 315 nm and emission at 400 nm). The *x* axis shows the elution time.

Table 1 Structure of tyrosinase and TRP-1 N- glycans

N-glycan structures released from tyrosinase and TRP-1 were analysed as shown in Figures 1 and 2. The data represent percentage molar ratio of total sugar chains released from each enzyme.

	Amount released (mol %)							
	High-mannose					Complex		
Type of glycan released ...	M5	M6	M7	M8	M9	A2G2	A3G3	A4G4
Tyrosinase	6.6	18.0	8.3	8.1	7.4	30.4	16.5	4.7
TRP-1	0.4	5.8	3.3	3.5	3.1	15.8	54.7	13.4

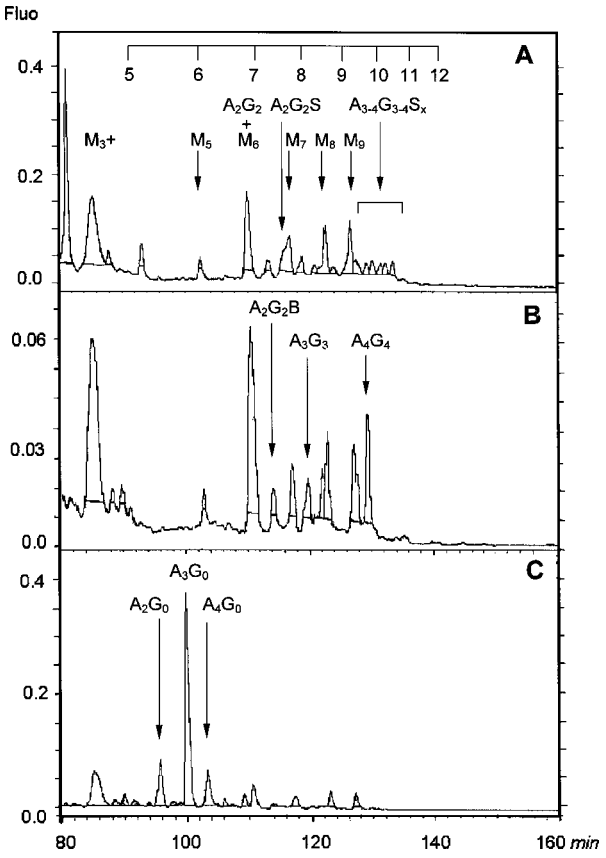

Figure 2 HPLC analysis of N-linked TRP-1 oligosaccharides digested with glycosidic enzyme arrays

The conditions are the same as those described in the legend to Figure 1.

N-glycans released from TRP-1 are presented in Figure 2. The profiles are similar to those of tyrosinase. However, the ratios between the different glycan structures are different in the two glycoproteins, indicating differences in the degree of N-glycan processing. Digestion with sialidase + β-galactosidase shows a completely different distribution of high-mannose versus polylactosamine structures in TRP-1 (Figure 2C). The ratio high-mannose/complex glycans is 1:1 in tyrosinase and 1:5 in TRP-1 (Table 1). In addition, while biantennary lactosamine structures represent 58.5% of the polylactosamine tyrosinase sugars, the major complex glycans in TRP-1 are the triantennary lactosamines (64%), indicating a more advanced glycan processing of TRP-1.

N-glycan processing of tyrosinase and TRP-1 in B16 mouse melanoma cells

To understand the differences in the degree of maturation of the N-glycans in tyrosinase and TRP-1, we investigated the processing of the two enzymes along the secretory pathway.

B16 mouse melanoma cells were pulse-labelled with [^{35}S]-methionine and chased for the time periods indicated in Figures 3(A) and 3(B). Cell lysates were immunoprecipitated with αPep7 (Figure 3A) or αPep1 (Figure 3B) antisera which were raised against the specific carboxy-terminal fragments of tyrosinase and TRP-1, respectively. Samples were divided in two, and half of each sample was digested with EndoH and run next to a non-

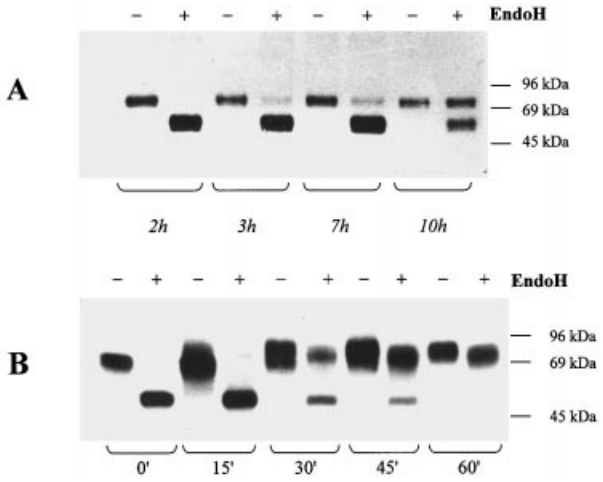

Figure 3 Processing of tyrosinase and TRP-1 N-glycans in B16 cells

B16 cells were pulsed for 30 min (**A**) and 10 min (**B**) with ^{35}S and chased for the indicated periods of time. Cell lysates were immunoprecipitated with αPep7 (**A**) or αPep1 (**B**) antiserum. The immunoprecipitates were divided in half and the two pools were digested (+) or not (−) with EndoH. The samples were run in SDS/PAGE 10% gel (**A**) or 7.5% gel (**B**) and visualized by autoradiography. The positions of molecular mass markers are shown on the right side of this and subsequent Figures.

digested control in reducing SDS/PAGE. Since EndoH digests only high-mannose and hybrid N-glycans, EndoH sensitivity was used to monitor the maturation of glycans from high-mannose to complex structures.

Tyrosinase is synthesized as a 72 kDa precursor totally sensitive to EndoH (Figure 3A). Digestion with EndoH reduces the pool to the polypeptide running at 60 kDa. During the first 2 h of chase the precursor has the same electrophoretic mobility and remains totally EndoH-sensitive. After 3 h of chase, digestion with EndoH is unable to completely reduce the ~ 72 kDa band. In addition, a new form resistant to EndoH is detected (Figure 3A). These results indicate that tyrosinase N-glycans are not extended to complex structures in the Golgi earlier than 3 h following biosynthesis. It is also interesting to note that a fraction of the mature tyrosinase remains sensitive to EndoH, revealing the presence of high-mannose/hybrid mature glycoforms of the enzyme. This can be clearly seen from the EndoH digest pattern at 10 h of chase (Figure 3A). Similar patterns were obtained on crude B16 melanosomal lysate and normal melanocytes after EndoH digestion [15,20].

TRP-1 is processed much faster than tyrosinase (Figure 3B). At 0 and 15 min chase TRP-1 is detected as a precursor totally sensitive to EndoH. Starting with 30 min of chase, TRP-1 presents a slightly slower mobility induced by N-glycan processing. Indeed, digestion of this sample with EndoH yields, in addition to the precursor form, an EndoH-resistant band corresponding to a complex type of glycoform. The maturation process of TRP-1 continues for another ~ 30 min with the progressive disappearance of the EndoH-sensitive TRP-1 form. Within 1 h of chase TRP-1 is completely processed, as shown by the disappearance of the precursor form (Figure 3B).

Inhibition of N-glycan processing in the presence of ER-glucosidase inhibitors

The occurrence of the EndoH-sensitive precursor form of tyrosinase and TRP-1 can be correlated with the time spent by these

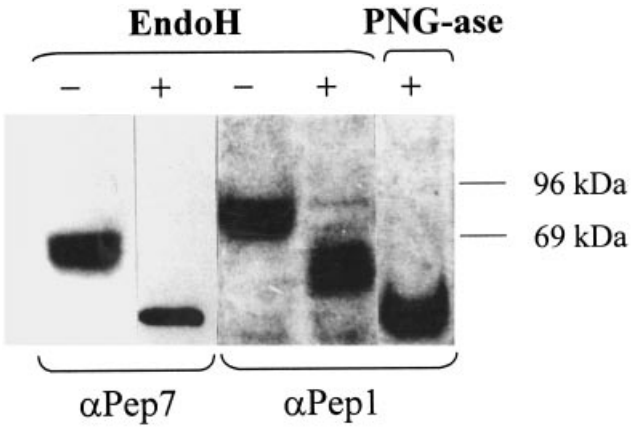

Figure 4 Western blotting of melanosomal tyrosinase and TRP-1 in NB-DNJ-treated cells

B16 melanosomal lysates obtained from cells cultivated for 72 h in the presence of 1 mM NB-DNJ were treated (+) or not (−) with EndoH or PNGase, separated by SDS/PAGE (7.5% acrylamide) and blotted. Tyrosinase and TRP-1 were detected immunochemically with αPep7 or αPep1 antisera, respectively.

glycoproteins in ER (and early Golgi). Thus further insights on the maturation process may be obtained by using inhibitors of the two exoglycosidases specific to this compartment, α-glucosidase I and II.

To investigate the mature glycoforms of the two enzymes, melanosomes from B16 cells cultivated in the presence of NB-DNJ have been isolated as described [15]. Melanosomal lysates were analysed by Western blotting with αPep7 and αPep1 antisera before and after EndoH digestion (Figure 4). Following EndoH digestion tyrosinase was converted into the polypeptide and no glycoform resistant to EndoH treatment could be detected. In contrast, melanosomal TRP-1 is partially resistant to EndoH, indicating that some of its glycans are further processed to complex structures (Figure 4).

The kinetics of TRP-1 N-glycan maturation in the presence of NB-DNJ were investigated by pulse–chase followed by immunoprecipitation (Figure 5). The cells were pulsed for 10 min and chased for 0, 15, 30, 45 and 60 min. The maturation rate is similar to that observed in untreated cells (Figure 3B). As in the untreated cells, TRP-1 appears at 0 and 15 min chase in its precursor form, totally sensitive to EndoH (Figure 5). At 30 min chase, treatment with EndoH results in several distinct bands, corresponding to glycoforms with different ratios of high-mannose and complex glycans. At 45 and 60 min chase a further increase of the EndoH-resistant form, with respect to the EndoH-sensitive population, is observed (Figure 5).

Dopa-oxidase activity in NB-DNJ-treated B16 cells

In non-denaturing SDS/PAGE B16 mouse melanosomal lysates show two bands with dopa-oxidase activity, referred to as LEMT and HEMT (for lower and higher electrophoretically migrating tyrosinase, respectively)[8]. These were inferred to correspond to TRP-1 and tyrosinase respectively. In B16 cells treated with NB-DNJ, dopa-oxidase activity decreases dramatically due to the inhibition of tyrosinase [15]. However, a residual activity could still be detected in these cells, even when high concentrations of inhibitor were used. Based on these observations we addressed whether the residual dopa-oxidase activity in NB-DNJ-treated B16 cells may be due to TRP-1.

To probe this hypothesis we worked on melanosomal rich fractions of untreated and NB-DNJ-treated B16 cells. Equal amounts of melanosomal lysates were run on SDS/PAGE under non-denaturing conditions, and the gel was incubated with dopa as described in the Experimental section (Figure 6). Untreated B16 crude lysate yields two bands with dopa-oxidase activity corresponding to LEMT (TRP-1) and HEMT (tyrosinase) as previously reported [8]. In contrast, in NB-DNJ-treated cells only one band with dopa-oxidase activity was observed. This band had a reduced mobility compared to TRP-1 (LEMT) from the untreated cells (Figure 6). Tyrosinase expressed in CHO cells displayed only one band with dopa-oxidase activity, and this band co-migrated with B16 tyrosinase (Figure 6). Unlike in B16 cells, in CHO cells transfected with tyrosinase cDNA and treated

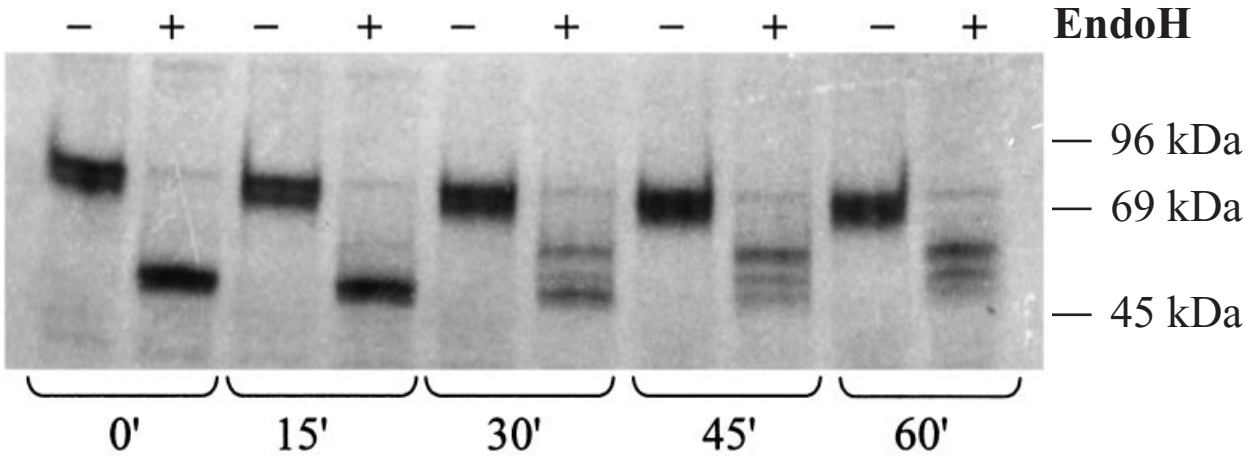

Figure 5 Processing of TRP-1 N-glycans in NB-DNJ-treated B16 cells

B16 cells were cultivated for 2 h in the presence of 1.0 mM NB-DNJ, pulsed for 10 min with ^{35}S and chased for the time periods indicated in the presence of the same concentration of the inhibitor. Cell lysates were immunoprecipitated with αPep1 antiserum and the eluted material divided in two, and each half digested (+) or not (−) with EndoH. Samples were separated by SDS/PAGE (7.5% acrylamide) and the proteins visualized by autoradiography.

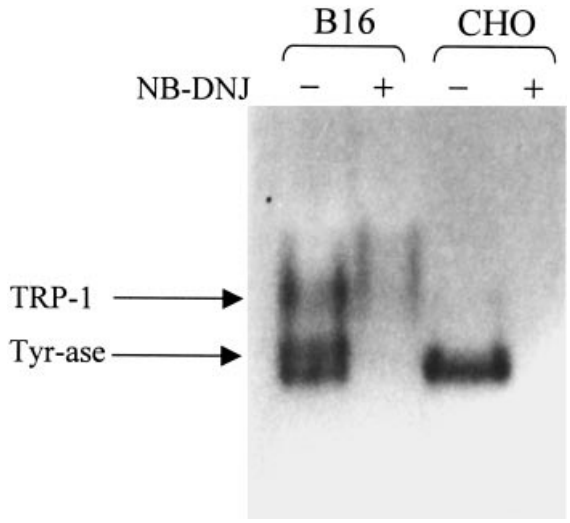

Figure 6 Effect of NB-DNJ on dopa-oxidase activity of B16 cells

CHO cells transfected with tyrosinase and B16 cells were treated for 72 h in the presence (+) or absence (−) of 1.0 mM NB-DNJ. Equal numbers (10^4) of cells were lysed, separated electrophoretically by SDS/PAGE (7.5% acrylamide) under non-denaturing conditions and stained for dopa-oxidase activity.

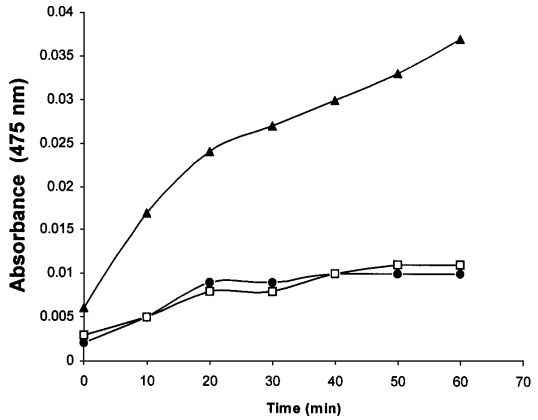

Figure 7 Dopa-oxidase activity in untreated, NB-DNJ-treated and tyrosinase-depleted B16 cells

B16 melanosomal lysate before (▲) and after (●) the removal of tyrosinase by immunoprecipitation with αPep7 antiserum or from NB-DNJ-treated cells (□) was tested for dopa-oxidase activity.

with NB-DNJ no residual dopa activity was detected (Figure 6). These results support the hypothesis that the residual dopa-oxidase activity in B16 cells comes from TRP-1. This hypothesis is further supported by the following experiment. The B16 melanosomal lysate was depleted of tyrosinase by immunoprecipitation with αPep7 antiserum and the dopa-oxidase activity was measured before and after immunoprecipitation. The activity of the lysate after removal of tyrosinase was compared with the residual dopa-oxidase activity detected in the NB-DNJ-treated melanosomal lysate. As Figure 7 shows, after removal of tyrosinase, dopa-oxidase activity significantly decreased and it was comparable with the activity detected in the NB-DNJ-treated sample in which tyrosinase was present but was enzymically inactive.

These results strongly suggest that in B16 cells in which TRP-1 has a dopa-oxidase activity, it might not be totally affected by inhibition of the N-glycan processing step with NB-DNJ as was observed for tyrosinase.

DISCUSSION

Processing of N-linked glycans has been shown to depend on the cellular control of glycosylation [21]. A subtle relation also exists between N-glycan processing, folding and the three-dimensional structure of glycoproteins. ER processing of N-glycans influences glycoprotein folding, whereas the glycoprotein architecture determines, in later stages, glycan processing in the Golgi. To investigate these intricate relations we have compared the folding kinetics and N-glycan processing of two closely related glycoproteins, tyrosinase and TRP-1, which share 40% sequence identity, are synthesized in the same B16 cell line, target the same organelle and are involved in the same metabolic pathway.

Despite similarities structural analysis reveals significant differences in the N-glycan patterns of the two glycoproteins. The processing of tyrosinase N-glycans is completed for 80% of the oligosaccharides before the development of complex triantennary structures. From the total pool 50% are high-mannose forms and 30% are complex biantennary. The presence of the oligomannosidic series has been also reported in hamster melanoma tyrosinase (Ohkura et al. [21a]). However the ratio of high-mannose versus complex structures is 1:3 in hamster, as compared to 1:1 in B16 tyrosinase. In contrast with tyrosinase, in TRP-1 only 16% of the glycans are of the high-mannose type, 16% are biantennary and 65% are extended to tri- and tetra-antennary structures. Another difference is that TRP-1 glycoforms contain mixtures of high-mannose and complex structures, while tyrosinase presents in addition a homogeneous high-mannose glycoform. The extent of N-glycan processing is limited by glycosidase availability in the Golgi and their accessibility to the processing sites. Clearly the availability is the same for the two glycoproteins; hence the difference in glycosylation indicates different accessibility, caused most probably by differences in the three-dimensional structures of tyrosinase and TRP-1.

There are also substantial differences in the kinetics of maturation of the two proteins. TRP 1 is processed in less than 1 h to its fully glycosylated form, whereas tyrosinase requires more than 3 h for complete maturation. Within the ER and early Golgi TRP-1 is detected for ~30 minutes, as shown by the EndoH digestion experiments. In contrast, tyrosinase is present in the same compartments for at least 3 h. These results are in agreement with our previously reported ER transit period estimated from the interaction of tyrosinase with calnexin, an ER-resident chaperone [22]. Tyrosinase and TRP-1 have been reported to display different maturation times in several cell lines, 2–3 h for TRP-1 and 3–6 hours for tyrosinase [20,23]. In the present study we compare directly the kinetics of N-glycan processing of the two glycoproteins in the same B16 cell line. Our results indicate that differences in the overall processing time of the two glycoproteins are due primarily to their ER residency and hence to their folding process rather than to their transport through the secretory pathway.

Insights on N-glycosylation functions were provided by experiments using inhibitors of the two ER α-glucosidases. These affect the N-glycan processing in the ER, and thus may interfere with the quality control system based on lectin-like chaperones such as calnexin and calreticulin. In the case of tyrosinase we have recently shown that there is an absolute requirement for calnexin in order for correct folding to occur. In the presence of NB-DNJ, tyrosinase does not interact with calnexin. In 30 min following

synthesis tyrosinase reaches the melanosomes in a misfolded, inactive state. Inactive tyrosinase lacks copper, indicating that the enzyme is misfolded in the region of the active site [22]. In contrast, we show here that the TRP-1 kinetics of transit is not changed in the presence of the α-glucosidases inhibitor. TRP-1 does not seem to have an absolute requirement for calnexin, although it can be immunoprecipitated by calnexin (G. Negroiu and S. M. Petrescu, unpublished work). Moreover, despite glucosidase inhibition, and hence in the absence of the interaction with calnexin, the dopa-oxidase activity of TRP-1 is only marginally affected. This suggests that, in contrast with tyrosinase, the TRP-1 conformation in the vicinity of the active site is not greatly affected by the perturbation of normal N-glycan processing.

It has been shown recently that copper incorporation into TRP-1 is reduced as compared to tyrosinase, and this correlates well with the low dopa-oxidase activity of TRP-1 [9]. It will be interesting to know if NB-DNJ treatment further reduces the already low TRP-1 copper content or if it induces other conformational modifications. Experiments on the copper content of TRP-1 in NB-DNJ-treated cells are in progress.

In the presence of NB-DNJ, the glycosylation pattern of tyrosinase is essentially uniform, with only $Glc_3Man_{7-9}GlcNAc_2$ structures being present [15]. In startling contrast, the glycosylation pattern of TRP-1 in the presence of the inhibitor contains oligosaccharides which are processed. One way the cell has of overcoming the glucosidase blockade is to use the endomannosidase pathway which acts in the Golgi and trims the three glucose and terminal mannose residues from the oligosaccharide moiety. It has been reported that the endomannosidase route is cell specific [24]. B16 cells appear to have an active endomannosidase, as shown by the processing of TRP-1 in the presence of NB-DNJ. However, our results suggest that although TRP-1 is a substrate for endomannosidase, tyrosinase is not. This raises the interesting and intriguing question as to whether the Golgi endomannosidase only acts on those proteins which are already correctly folded. It may well be that the misfolded proteins are such that the structure around the glycan moiety prohibits access of the endomannosidase.

In conclusion, our results show that inhibition of N-glycan processing in B16 cells has different effects on the N-glycan maturation and activity of the two closely related glycoproteins. Tyrosinase activity is completely inhibited, while the dopa-oxidase activity of TRP-1 is only slightly diminished. However the remaining dopa-oxidase activity of TRP-1 is not sufficient to initiate melanin synthesis *in vivo*. This again raises questions regarding the real function of TRP-1. The abundance of TRP-1 in melanocytes suggests that its role may be that of a structural protein in maintaining the integrity of the melanosomes or the stability of tyrosinase [25] rather than as an enzyme. In this case one would expect the two TRPs to adopt different conformations according to their specific functions. The different glycosylation of the two proteins provides an interesting probe into the exact mechanism of protein folding, clearly pointing to the need for further examination of the relationship between the Golgi endomannosidase, the glucosidases blockade and the protein folding.

Received 13 July 1999/7 September 1999; accepted 8 October 1999

We thank Dr. V. J. Hearing (National Institutes of Health, Bethesda, MD, U.S.A.) for anti-tyrosinase and anti-TRP-1 antisera. This work was supported by grants from the Wellcome Trust (Collaborative Research Initiative Grant no. 053441), the Romanian Academy and the Romanian Ministry of Research and Technology.

REFERENCES

1 Hearing, V. J. and King, R. A. (1993) in Pigmentation and Pigmentary Disorders, part 2 (Norman, L., ed.), pp. 5–31, CRC Press, Boca Raton
2 Muller, G., Ruppert, S., Schmid, E. and Schultz, G. (1988) EMBO J. **7**, 2723–2730
3 Hearing, V. J. and Ekel, T. M. (1976) Biochem. J. **157**, 549–557
4 Kobayashi, T., Vieira, W. D., Potterf, B., Sakai, C., Imokawa, G. and Hearing, V. J. (1995) J. Cell Sci. **108**, 2301–2309
5 Jimenez-Cervantes, C., Solano, F., Kobayashi, T., Urabe, K., Hearing, V. J., Lozano, J. A. and Garcia-Borron, J. C. (1994) J. Biol. Chem. **269**, 17993–18001
6 Boissy, R. E., Sakai, C., Zhao, H., Kobayashi, T. and Hearing, V. J. (1998) Exp. Dermatol. **7**, 198–204
7 Jimenez, M., Tsukamoto, K. and Hearing, V. J. (1991) J. Biol. Chem. **266**, 1147–1156
8 Jimenez-Cervantes, C., Garcia-Borron, J. C., Valverde, P., Solano, F. and Lozano, J. A. (1993) Eur. J. Biochem. **217**, 549–556
9 Furumura, M., Solano, F., Matsunaga, N., Sakai, C., Spritz, R. A. and Hearing, V. J. (1998) Biochem. Biophys. Res. Commun. **242**, 579–585
10 Petrescu, A.-J., Butters, T. D., Reinkensmeier, G., Petrescu, S., Platt, F. M., Dwek, R. A. and Wormald, M. R. (1997) EMBO J. **16**, 4302–4310
11 Kornfeld, R. and Kornfeld, S. (1985) Annu. Rev. Biochem. **54**, 631–664
12 Zapun, A., Petrescu, S. M., Rudd, P. M., Dwek, R. A., Thomas, D. Y. and Bergeron, J. J. (1997) Cell **88**, 29–38
13 Elbein, A. D. (1987) Annu. Rev. Biochem. **56**, 497–534
14 Dairaku, K. and Spiro, R. G. (1997) Glycobiology **7**, 579–586
15 Petrescu, S. M., Petrescu, A.-J., Titu, H. N., Dwek, R. A. and Platt, F. M. (1997) J. Biol. Chem. **272**, 15796–15803
16 Aroca, P., Urabe, K., Kobayashi, T., Tsukamoto, K. and Hearing, V. J. (1993) J. Biol. Chem. **268**, 25650–25655
17 Jimenez-Cervantes, C., Valverde, P., Garcia-Borron, J. C., Solano, F. and Lozano, J. A. (1993) Pigment Cell Res. **6**, 394–399
18 Petrescu, S. M., Branza-Nichita, N., Nita-Lazar, M., Petrescu, A.-J. and Motas, C. (1995) Anal. Biochem. **229**, 299–303
19 Guile, G. R., Rudd, P. M., Wing, D. R., Prime, S. B. and Dwek, R. A. (1996) Anal. Biochem. **240**, 210–226
20 Halaban, R., Cheng, E., Zhang, Y., Moellmann, G., Hanlon, D., Michalak, M., Setaluri, V. and Hebert, D. N. (1997) Proc. Natl. Acad. Sci. U.S.A. **94**, 6210–6215
21 Rudd, P. M. and Dwek, R.A (1997) Curr. Opin. Biotechnol. **8**, 488–497
21a Ohkura, T., Yamashita, K. and Mishima, Y. (1984) Arch. Biochem. Biophys. **235**, 63–67
22 Branza-Nichita, N., Petrescu, A.-J., Dwek, R. A., Wormald, M. R., Platt, F. M. and Petrescu, S. M. (1999) Biochem. Biophys. Res. Commun. **261**, 720–725
23 Vijayasaradhi, S., Xu, Y. Q., Bouchard, B. and Houghton, A. N. (1995) J. Cell Biol. **130**, 807–820
24 Karaivanova, V. K., Luan, P. and Spiro, R. G. (1998) Glycobiology **8**, 725–730
25 Kobayashi, T., Imokawa, G., Bennett, D. C. and Hearing, V. J. (1998) J. Biol. Chem. **273**, 31801–31805